A Visible Light Terrestrial Planet Finder --Planet Detection and Spectroscopy by Nulling Interferometry with a Single Aperture Telescope

B.M. Levine, Michael Shao, C.A. Beichman, B. Mennesson, R. Morgan, G. Orton, E. Serabyn, S. Unwin, T. Velusamy,
Jet Propulsion Laboratory/California Institute of Technology
4800 Oak Grove Drive
Pasadena, CA 91109-8099
and
N. Woolf
University of Arizona, Seward Observatory, Tucson, AZ

Keywords: **Visible Light Planet Detection, Nulling Interferometer, Coronagraph**

Abstract

Planet detection around a bright star depends the resolution of the imaging system and the degree of light suppression of the star relative to the planet. We present a concept for a visible light Terrestrial Planet Finding (VTPF) mission. Its major feature is an imaging system for planet detection using a nulling interferometer behind a single aperture telescope. This configuration is capable of detecting earth-like planets with a 5m aperture using both imaging and spectroscopic imaging modes. We will describe the principles of the system, and show results of studies demonstrating its feasibility.

Introduction

The detection of extrasolar planets does not, in principle, require large collecting areas for either resolution or photometric purposes. If we view our solar system from 10 parsec in the visible, a Jupiter-like planet has an approximate magnitude of V~27 and the Earth is V ~ 30. The Hubble Space Telescope (D=2.4m) can detect a V = 30 object, so a 27 magnitude object takes much less than 1 hr of integration. In terms of resolution a Jupiter-like planet at 10 parsec subtends an angle of 0.5 arc seconds, which requires a diffraction limited telescope of only 30cm or greater (at 0.75μm wavelength) .

With a flux ratio in the optical of ~10^9 between a planet and its star, the harder problem is that of contrast. Achieving a very low background against which to detect a planet requires control of both scattered and diffracted light. Adaptive optics (AO) coronagraphs (Malbet, Yu, and Shao, 1995) provide a partial solution, by using a deformable mirror to improve the wavefront quality and create a 'dark hole' at the center of the field of view, effectively improving the telescope Strehl. Effectively, the deformable mirror reduces the scattering or mid spatial frequency errors that cause spurious scattering into the region where the planets would be found. In the recent studies for TPF, four teams studied numerous concepts for direct detection of planets including coronagraphs and apodized aperture telescopes. For the detection of an Earth-like planet in the visible, around a Sun at 10pc, a *large* telescope (~8-10m diameter) was recommended to place the planet at least 3-4 Airy rings from the star. The size of the aperture is needed to spatially separate the star from the planet but unnecessary for the fundamental task of collecting photons from the planet.

A nulling interferometer, however, can be used to suppress both diffraction and scattering, and it can be located behind a much smaller aperture to resolve an extrasolar planet. A nulling interferometer effectively cancels the starlight and has 100% transmission for planet light when the optical path from the planet is $\lambda/2$ different from the star. For our concept this corresponds to $\theta = \lambda/b$ (b= interferometer baseline). By contrast a coronagraph operates out at several Airy rings (~ 3-4 x $1.22\lambda/D$). For a modest sized aperture, say D=1.5m, a Jupiter-like planet could be resolved by synthesizing an interferometer with a 30 cm baseline.

This paper describes a new instrument for direct planet detection. It synthesizes a four element nulling interferometer from the telescope pupil to suppression the diffraction from the central star. After nulling, an array of coherent single mode optical fibers is used provide the scattering suppression to negate the effects of residual stellar leakage due to imperfections in the telescope optics and optical train. A simple imaging system after this array forms the final extrasolar planet image. This concept combines all the advantages of a nulling interferometer with the simplicity of a modest size and modest optical quality single aperture telescope. Such a telescope with the new nulling interferometer as back-end instrument can image and detect planets, or provide the input to a low resolution spectrometer. Its a primary optic is at least two times smaller in diameter (4 times in area) than a traditional adaptive optics coronagraph, which potentially translates to a proportional savings in cost. The schematic system is shown in Figure 1.

Advances in nulling technology enable this approach. The SIM testbed nuller, has demonstrated 99.999% stabilitzed nulls and 99.9999% transient nulls. Over the last 3~4 years, nulling technology at the Keck Interferometer, the MMT, the LBT interferometer, and SIM ground support testbeds has come very close to what is

needed for planet detection in space. A further key element of the nulling approach is the use of single mode fiber spatial filter in conjunction with the nulling interferometer. This combination makes very deep nulling possible without λ/4000 wavefront quality over a large full aperture.

Science justification for future missions

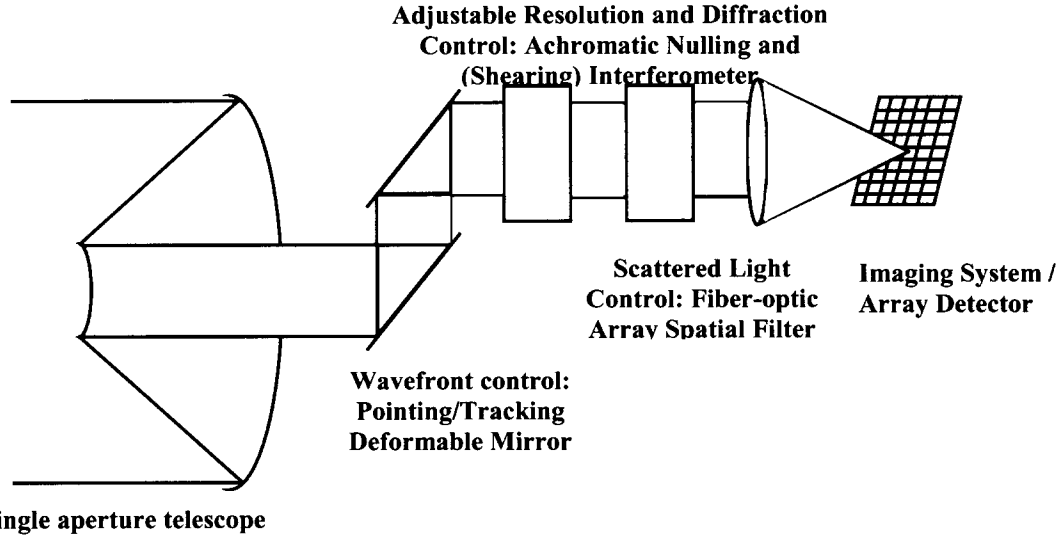

Figure 1: General layout for planet finding using a nulling interferometer and fiber-optic array.

Over 100 planets around nearby stars have already been discovered by radial velocity techniques (RV). RV methods can measure the planet's orbital period, radius, eccentricity, and $M\sin(i)$. Using this concept, direct detection provides the next layer of information. Such an Optical Planet Discoverer (OPD) mission would demonstrate the *scientific* feasibility of this approach using a modest sized aperture, for detection and spectroscopy of Jupiter-like planets. It would also demonstrate technical feasibility as well, because it would observe in the same band (optical), using the same basic instrument design, and same observing method, as the 'ultimate' visible TPF (VTPF) mission for the detection of earth-like planets. Scientific 'test targets' are already known. As we discuss later, several of the extrasolar planets already known from radial-velocity monitoring have planets should be readily detectable. Providing a low-resolution spectrometer is a highly valuable feature even if spectroscopy can be achieved only for the brightest detections thus demonstrating *the first physical characterization* of the atmospheres (or surfaces) of planets beyond our own solar system. Currently, an IR interferometer TPF concept would detect the 11-μm ozone feature in an exo-Earth's atmosphere. But visible spectroscopy of an exo-Earth is equally fascinating and complementary to an infrared mission. A visible nulling interferometer behind a 4-m class telescope could also search 100's of nearby stars within 15 pc of the Sun for Earth-like planets in the habitable zone. This is consistent with the long-term science objective to study exo-planets in both the visible and IR spectral bands.

If we view our solar system from a large distance, Earth appears only 6.6 times fainter than Jupiter. Since our detection sensitivity is limited by scattered starlight, even if a '47 UMa' planet had a density as high as Earth's (unlikely), it would still be readily detectable. Several others of the currently known extrasolar planetary systems, such as Ups and d, 16 Cyg b, and HD 160691, have orbit sizes in the peak sensitivity range for OPD. For stars closer than 10 pc, our peak sensitivity lies in the ~1-AU range. Note however, that these are all long-period planets, with P >~ 2 years. These estimates demonstrate that detection of Jupiters is well within the reach of OPD, and that with longer integration times, small-diameter planets should also be detectable.

What can be determined from low-resolution spectroscopy

Low-resolution ($R = \bar{\lambda} / \Delta\lambda \sim 20$) spectroscopy of resolved planets in the spectral region 500-1000 nm may enable critical additional physical and chemical characterization. Even qualitative information can be obtained from relative reflectivity spectra without requiring an absolute albedo scale. These additional properties will impose valuable constraints on models for planetary formation and evolution.

A straightforward example is differentiating between gas giant and terrestrial planets in our Solar System (Figure 2). These spectra are strikingly different: even with low SNR, and modest spectral resolution ($R = 20$) these spectra would be easily separable with OPD. It is easy to distinguish terrestrial and giant planets using 500-1000 nm spectra, because of the unmistakable absorption bands of methane (CH_4), the most prominent of which is at 890 nm, evident in Jupiter and Neptune.

The absence of spectroscopic methane does not necessarily imply that the body is a terrestrial planet. Figure 2 also shows a spectrum for an extrasolar giant planet (EGP) (Sudarsky et al. 2000), representing one of the hottest models of a suite ranging from Jupiter-like to 'roasters'. This particular EGP model illustrates absorption features of

CH_4 and H_2O between 890 and 1000 nm, as well as electronic transitions of ionized Na near 700 nm and K near 800 nm. Electronic features and the presence of H_2O form a useful 'thermometer' to gauge the high-temperature end of possible EGP conditions. In other models, the presence of gaseous absorption features is partially obscured by high-level clouds which diminish the effective optical path length. These high-temperature spectra might be expected of gas giants located extremely close to their primaries.

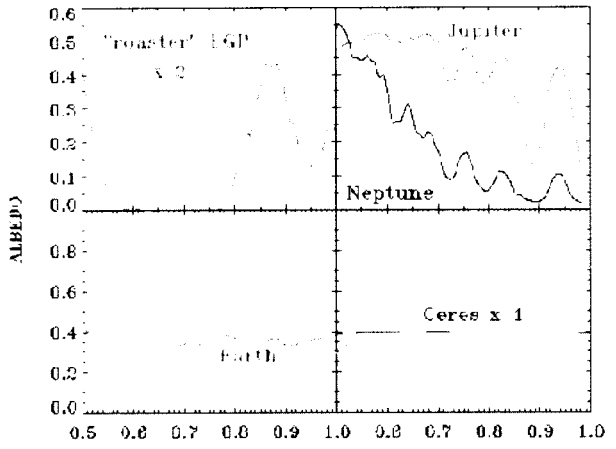

Figure 2: Predictions and observations of planetary spectra for visible light.

The spectrum of the earth shows evidence of atmospheric scattering in the rise of the spectrum going from 0.6 to 0.5μm The spectrum of the Earth shows two of the critical signatures in NASA's search for evidence of life:

(i) water vapor absorption bands at 0.92μm (with fainter ones at 0.72 and 0.82μm),

(ii) a narrow band of O_2 near 0.76μμ that might be resolved above the signal level, and (iii) a spectral "vegetation edge" rising from 0.6 to 0.7μm which is due to absorption by green foliage.

An exciting prospect for the full scale VTPF mission, if not for OPD itself, would be to search the highest SNR detected planets for spectral variability due to rotation. If large variations in, say, cloud cover or depth exist, they should be detectable.

Planetary system inventory, demographics and planetary system dynamics

The fraction of G and K stars with Jupiters is already fairly well established at ~7%, for radii less than a few AU, and masses greater than ~0.5 Jupiters. But what fraction of early-type stars has 'Jupiters', relative to late-type? Prior to OPD, this may be partially answered by the French stellar photometry mission COROT (with very limited statistics) or with microlensing. COROT will be limited to short-period systems ($P < 50$ days), while OPD will sample planets with larger orbit radii.

OPD will allow us to explore a range of stellar types. Unlike precision RV studies, direct detection will work for *any* stellar type. The contrast ratio is not, to first order, a function of the stellar magnitude. By studying different stellar types, we can learn many things: How is the mass in planets related to the star's mass? Is the distribution of planetary masses and orbit radii (for the largest one or two planets in each system) a function of stellar type? How does a star's age, or evolutionary state, affect its planetary system?

Massive planets in long-period orbits are believed to stabilize the inner planets, based on our own solar system, and N-body simulations (Levison et. al. 2001). OPD will find such systems, if they exist, and hence form target list for VTPF. These are mostly *not* the systems detected by current RV programs. For instance, the 51-Peg systems are not conducive to searches for Earths, because the formation and evolution of such systems appears to preclude the presence of an Earth in a circular orbit potentially stable for a billion years. Likewise, the systems with Jupiters at larger radii show eccentric orbits, and a significant fraction are probably interacting strongly. Secular resonances are seen in HD 83443 (Wu & Goldreich 2001); and GL 876 (Lee & Peale 2001). OPD will provide crucial data by measuring the orbit inclinations and longitudes of ascending nodes. Even without accurate masses, these data would allow very detailed simulations of long-term system stability, which are important for the longevity of Earths. OPD will push to lower mass planets; as the role of Neptune-mass planets in stabilizing an inner-planet zone is currently unknown.

For planets detected in short-period orbits (<1 - 2 years) we can study dynamics, by tracing enough of the orbits to solve for Keplerian parameters. Orbit fits must include illumination phase, hence allowing an estimate of the 100% illumination brightness. In particular, since we are constrained to orbit radii less than a few AU, we will be in the sensitivity range of the RV studies. OPD complements the ground-based radial velocity work, by detecting planets at similar orbital radii. Combining RV data with detection by OPD provides a very complete picture of the planetary system: all 7 orbital elements; planetary mass, and (for an assumed albedo) radius and density also.

Nulling System Design

The most challenging technological problems are those concerning suppression of starlight in the resulting image. Deep stellar nulling requires a broadband, stable subtraction scheme, so the residual limitations inherent in earlier designs need to be overcome. These limitations have been identified, and can be obviated by simply using a reversed pair of beam splitters. Additional suppression is gained by filtering off-axis, high spatial frequency star light. This has been successfully used in the past in interferometry (Serabyn et.al., 1999), and has recently been suggested in the literature for planet detection (Mennesson, Ollivier & Ruilier 2002.

Nulling Description and Interferometer Layout

As part of the earlier SIM technology development effort, an optical nulling testbed was developed at JPL. The approach used was that of an achromatic field flip introduced between the two incident beams by means of a rotational shearing interferometer (Shao and Colavita 1992). Although this nuller met and even exceeded the nulling performance requirements set for the SIM mission, its requirement was eliminated from the mission. With laser sources, transient nulls exceeding 1,000,000:1 and stabilized nulls of 100,000:1 were obtained, while with a broadband thermal source, broadband radiation of 18% bandwidth was stably nulled to the 10,000:1 level, with transient nulls of up to 70,000:1 seen (Wallace et. al, 2000). Several limitations have been further identified in the approach. Residual asymmetries in the interferometer layout limited the ultimate null depths attainable: unequal numbers of anti-reflection-layer traversals, unequal reflections from opposite sides of the beamsplitter coating, and polarization asymmetries in the beamsplitter. All have been eliminated in the current design. A further important simplification arises if one considers a separation of the field-flip and beam-combination stages. These considerations led to the emergence of a fully symmetric nuller design (Serabyn and Colavita 2001) using a simple constructive Mach-Zehnder-like beam combiner. Because of the complete symmetry of this design, substantially improved performance is expected, allowing even deeper and more broadband nulls, as well as dual-polarization nulls. A related modified Mach-Zehnder approach is being developed in the thermal infrared for use in the Keck Interferometer nuller. For this mission, we have chosen the single input versions as differentiated from designs used to combine light from two physically separate arms of an interferometer (Figure 3).

Our principal concept is to synthesize a 4 element interferometer from the telescope pupil. arranged in an 'Angel cross'(Angel, 1990). This is accomplished with two nulling interferometers (Shao, 1990, Serabyn and Colavita, 2001) that also shear the pupil. With coupling optics between the two nullers that rotates the pupil by 90°, the final output pupil looks like Figure 4. The resulting nulled output is then spatially filtered by an array of optical fibers. The shear distance provides the interferometer baseline, the nulling cancels the starlight by destructive interference, and the fiber array spatially filters the scatter yet preserves the pupil geometry. An imaging system transforms the resultant nulled pupil into either an image or a spectrum.

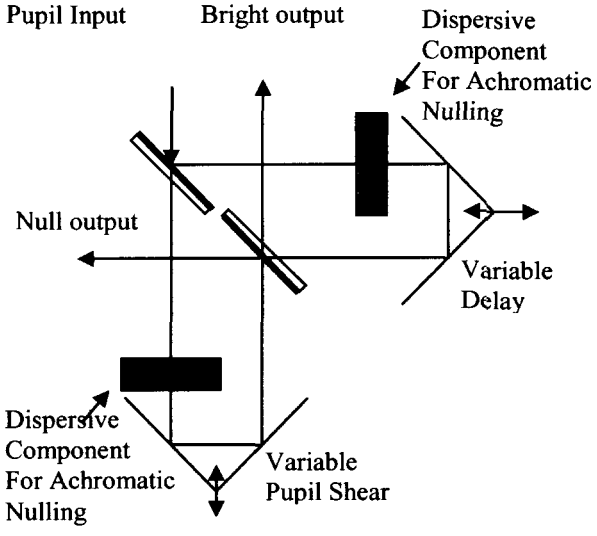

Figure 3: Nulling interferometer layout.

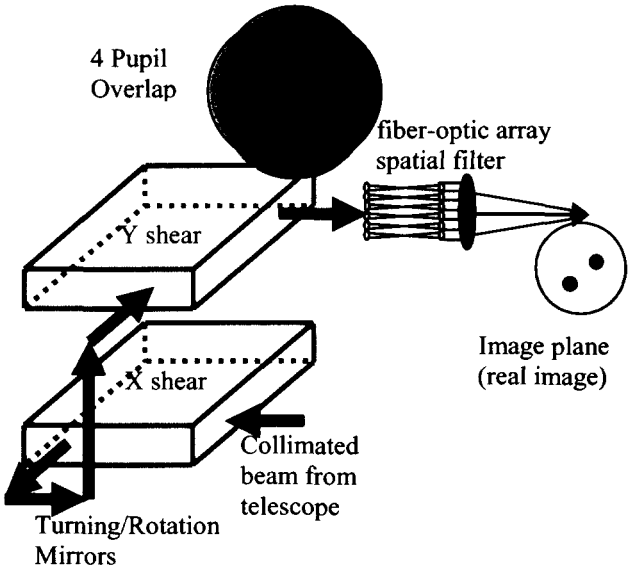

Figure 4: Pupil shear pattern and image formation using two nulling interferometers.

Performance and sensitivity considerations

Required null depth N.

Whereas a conventional 2 beam interferometer with a projected baseline, b, and with wave number, $k= 2\pi/\lambda$ produces a nulled fringe intensity proportional to θ^2, where θ is the angle from the optical axis,

$$I \propto (kb)^2 \theta^2$$

the 4 subapertures produce an intensity proportional to θ^4 thus deepening the null from the star and enhancing the intensity of the reflected light from the planet (Angel and Woolf, 1997, Mennesson and Mariotti, 1997)

$$I \propto (kb)^4 \theta^4 .$$

The aditional angular suppression is needed to provide a sufficiently deep null over the spatial extent of a star similar to the sun (1mas). This pattern is shown in Figure 5 below for both a narrow and extended field of view.

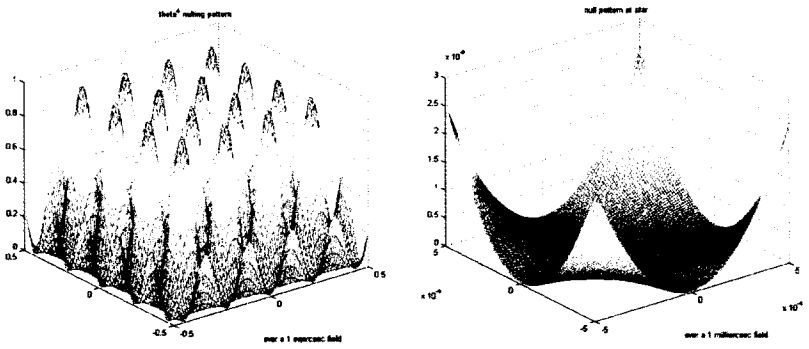

Figure 4: Intensity response of a four element nulling inteterferometer. Left, fringe pattern over a 1 as field of view. Right, nulling depth over 1mas, the angular extent of a sun at 10pc.

Further starlight suppression is accomplished by sampling the nullled subaperture by an array of microlenses and filtering the light via single mode optical fibers (Shao, 1990). Recollimation by a similar lens array provides a corrected exit pupil, and imaging by a simple achromatic lens produces the final nulled image of the planetary system. The basic idea and major advantage to this design is that no active wavefront correction is required for spatial scales smaller than the size of the lenslet. This is due to using single mode optical fiber. On the otherhand, using an array of fibers at the 5cm scale at a pupil guarantees a 2" field of view for nulling imaging. The main figure of merit for a nulling interferometer is its rejection rate. It is defined as the ratio of constructive to destructive intensity signals as obtained on a source of given characteristics (spatial and spectral extent for instance). Even for perfect pointing and perfect wavefront quality, the interferometric transmission is only zero on the line of sight, so that a star of finite angular size will always produce leaks limiting the rejection rate. This is referred as residual "stellar leaks" or limited "null depth" N. In practice, null depths as low as 10^{-7} are necessary to compensate for the large contrast ratio between stellar and planetary visible fluxes.

Entrance pupil shear

In order to efficiently reject the stellar light, we propose subdividing the entrance pupil into 4 sub-apertures to be nulled out according to an Angel cross (Angel 1990) recombination scheme. Defining b as the baseline between sub-apertures centers in a pair, assuming perfect pointing, and integrating the leaks over a uniform stellar disk of full angular extent $\Delta\theta$, the theoretical null depth N is given by:

$$N(\Delta\theta) = \frac{1}{2048}(\pi.b.\Delta\theta/\lambda)^4$$

Normalizing to the case of a 1mas diameter star (a Sun at 10pc has an apparent diameter of 0.9mas), seen at 500nm, with sub-apertures separated by 1m, we get:

$$N = 4.2\,10^{-10}.(\Delta\theta^*_{mas})^4.(\frac{500}{\lambda_{nm}})^4.(b_m)^4$$

Ensuring stellar leaks smaller than $5x10^{-8}$ at 500 nm on Procyon (closest F star) which is about 3mas in angular diameter requires a separation, b, smaller than 1m. This is consistent with forming 4 sub-apertures in the 60 to 80cm diameter class out of a 1.5m class telescope as suggested for OPD, the precusrsor mission concept. A full VTPF mission based on a visible nuller concept uses a larger primary mirror, typically 4m in diameter would need only a small amount of shear so that the closest stars are not too resolved.

Achromatic Nulling Beam Combiner

The symmetric nuller as currently used does have one limitation for this application that being that a field flip is accompanied by an aperture inversion. For the sub-aperture sampling described here, this results in undesirable shifts in location of the combining subapertures. To avoid this, it is necessary to introduce the necessary achromatic π-radian phase shift in a different fashion, such as pairs of dielectric plates of differing thicknesses. Solutions for achromatic π-radian phase shifts (to the needed accuracy) exist with two glasses. Thus for this experiment, the final layout for the beam combiner consists of identical two-glass pairs of (rotatable) dielectric phase retarders (Morgan et. al. 2000, Morgan 2002), in each leg of the interferometer. Note that the combination of common BK7 and Fused Silica optical glasses the theoretical minimum of 10^{-7} can be realized. This design will be verified in laboratory experiments.

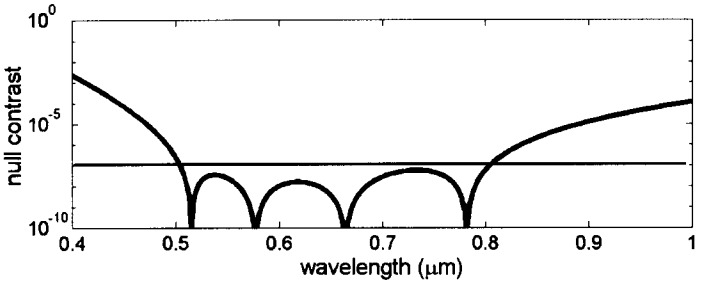

Figure 5: Calculation for nulling depth for common optical glasses, BK7 and Fused Silica.

lenslet pupil diameter requirements.

The injection of a stellar wavefront into a single-mode fiber is optimized for an f-ratio that matches the Airy spot and fiber core sizes. If only one common fiber were used to clean the wavefront, the field of view would then be limited to a sub-aperture Airy pattern. In order to keep some reasonable field of view together with the advantages of spatial filtering, the nuller output pupil is subdivided in lenslet pupils of diameter l, which are imaged onto an array of single-mode fibers via a lenslets array. The accessible field of view is now λ/l, so that lenslet pupils smaller than 5 cm guarantee a 2 arcsec diameter field of view at any $\lambda >$ 500nm. This is enough to detect Jupiter analogs around the closest main sequence stars. Using sub-apertures diameters ranging from 60 cm to 80 cm, an array of 100 to 200 fibers is needed.

Single-mode fibers

The light coming from the 4 sub-apertures is first mixed at the nulling beam combiner level. An array of lenslets, hexagonally packed, is then used to focus the resulting light onto an array of single-mode fibers. After propagation through these waveguides, the beams are recollimated with a matching lenslet array, and a final image is formed. The single-mode fiber filtering effect allows to get rid of all wavefront distortions at the 5cm lenslet pupil size level, and smaller. Single-mode fibers basically trade all local amplitude and phase mismatches (besides piston) between the recombined wavefronts against global intensity mismatches. Intensity mismatches are of secondary effect on the null depth. Thanks to this property, the instrumental null depth no longer varies as σ^2_φ the wavefronts initial phase variance, but as σ^4_φ (Mennesson et al. 2002), or even better if active intensity correction is implemented. For a given wavefront amplitude and phase profile, much deeper stellar light cancellation is then achievable when single-mode waveguides are used (Shao 1991). Single-mode fibers also have the advantages of broad-band utilization; the injection efficiency is roughly achromatic over an octave, and perfect amplitude profile matching of the wavefronts to be nulled out. Polarization maintaining silicon based single-mode fibers are well developed in the visible to near infrared wavelengths and widely used in observational astronomy.

Nulling requirements

The fraction of stellar photons leaking through the final focal plane at the planet's image location, needs to be kept below 10^{-8} for sensitivity reasons. Residual stellar light is expected to be coherent after its path through the array of single-mode fibers so that its energy distribution concentrates at the center of the final focal plane, and drops rapidly from there. Owing to this spatial dilution effect, rejection ratios around 10^{7} (i.e. null depths of 10^{-7}) will be enough to reach the above 10^{-8} level for any planet located further than 150mas away from the star.

Imaging optics

Once the stellar light has been cancelled at the 10^{-7} level in the array of fibers, requirements for downstream imaging optics are considerably relaxed. Fiber lengths and differential pistons between lenslet pupils need to be matched within $\lambda/20$ (but with higher stability) to ensure sufficient image quality and stability in the final focal plane. Observations with the visible nuller are made by either a CCD camera or a spectrometer. A movable mirror could allow to choose between the 2 instruments.

Low resolution spectrometer

Once planets have been detected and located with maximum sensitivity, a movable mirror sends the scientific beam towards a spectrometer. Two types of spectrometers are being considered, one is a "long" slit spectrometer, where the slit direction is aligned in the direction of maximum planet throughput. The second is an integral field spectrometer that would measure the spectra of every object in the field.

In the latter case, an image is formed on a 2-dimensional bundle array of 1500 multi-mode fibers. These are rearranged along one direction to allow spectral dispersion in the perpendicular one. A final CCD matrix using 1500 pixels in the spatial dimension and 15 in the spectral one is enough to carry-out integral field low resolution (20) spectroscopy in the 500-1000nm range.

Performance Studies

Integration times for broad-band planetary detection and spectroscopy

Broadband planetary detection would be carried out over the whole 500-1000nm spectral range. We derive in the following the integration times necessary to detect Jupiter and Earth analogs around nearby stars of various types, using respectively a 1.5m telescope (Discovery class mission nuller) and a 5-m extended capability (full TPF nuller). For a Jupiter sized planet the integration time goes as:

$$T_{int} = 14.3\ hr\ .\left(\frac{SNR}{5}\right)^2.\left(\frac{1.5}{D}\right)^2.\left(\frac{0.05}{eff}\right).\left(\frac{sl}{10^{-8}}\right).\left(\frac{Dist_{in\,pc}}{10}\right)^2.\left(\frac{Reso}{1.4}\right).\left(\frac{Sep}{5.2}\right)^4.\left(\frac{F_{sun}}{F^*}\right)$$

And similarly, the integration time for imaging a Sun-Earth system is:

Figure 6 summarizes the required integration times for detection of Jupiter and Earth analogs around stars of variable spectral types located 10 pc away, with nominal values for the observing parameters as noted.

$$T_{int} = 57.4\ hr\ .\left(\frac{SNR}{5}\right)^2.\left(\frac{5}{D}\right)^2.\left(\frac{0.05}{eff}\right).\left(\frac{sl}{10^{-8}}\right).\left(\frac{Dist_{in\,pc}}{10}\right)^2.\left(\frac{Reso}{1.4}\right).\left(\frac{Sep}{1AU}\right)^4.\left(\frac{F_{Sun}}{F^*}\right)$$

The integration times were all computed as a function of solar flux and reflected flux, planet albedo, stellar leakage. Once a planet has been detected, telescope rotation angle may be chosen to place it on a constructive fringe and carry out spectroscopic analysis with optimized sensitivity around a given wavelength. We further show in Table 2 the required integration times using our system while observing known planetary systems.

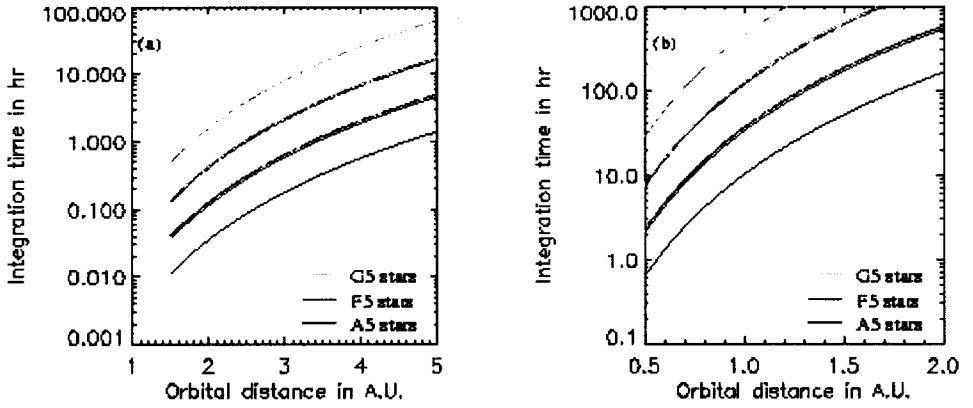

Figure 6 (a): Integration times for 5σ detection of Jupiter analogs around main sequence stars of various spectral types located 10pc away. Plain curve: broad-band (500-1000 nm) detection. Dotted curves: narrow band ($R \sim 20$) detection, Reso= $\frac{\lambda}{\Delta\lambda} = \frac{0.70\mu m}{0.5\mu m} = 1.4$, the spectral resolution. Telescope diameter, D, is 1.5m, *eff*, the overall optical efficiency (including primary area filling factor, optics transmission and detector quantum efficiency) is 5%, interferometric off-axis point-source transmission is 25%. The fraction of stellar leakage, *sl*, at planetary location: 10^{-8}. *Dist* is the stellar distance in pc, *Sep,* is the star-planet separation in au, and F denotes the appropriate body flux. (b): Similar plot for Earth-like planets using a 5m telescope. Solid lines denote imaging and the broken lines denote spectoscopic observations.

Figure 9 shows the brightness of the planets and the effect of the stellar leakage in the image for a star 10pc and for a nearby star e-Eri (3.3pc). Note that the planet fluxes are averaged over all orientations of the null pattern. Spectral studies will be made at a single orientation at which the observed flux can be much higher. The effects of the stellar leakage, therefore, is not a serious problem.

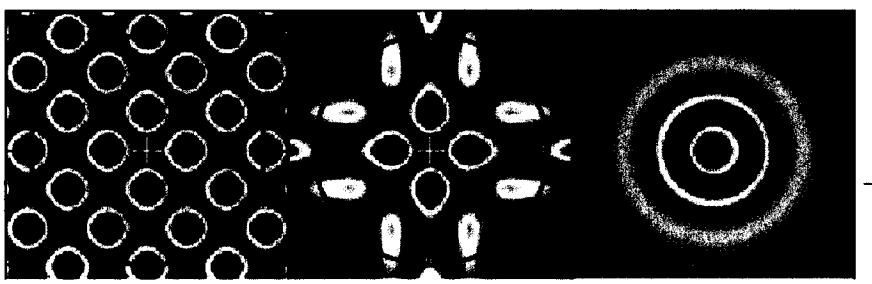

Figure 7: The null response pattern of OPD. (left) at wavelength 650nm and at

one orientation. (middle) Using wavelengths 500-1000nm and at one orientation.(right) Using wavelengths 500-1000nm and combining all orientations 0-360deg. The circle represents 5AU radius at 10pc distance. Response maxima are shown in red.

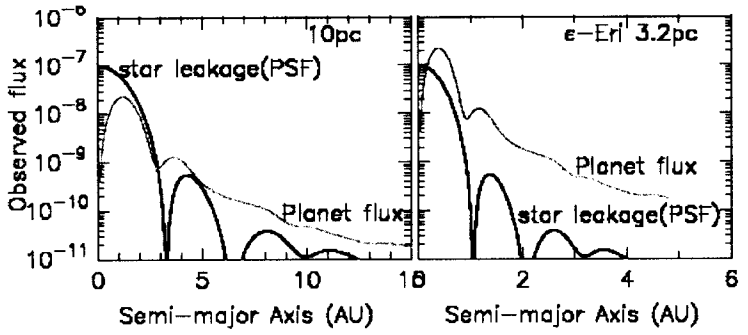

Figure 8: Observed planet fluxes compared to the PSF of the stellar leak as a function of the planet distance. Null depth of 10^{-7} was assumed. The planet flux densities are assumed to be that for Jupiter size and given in units of stellar flux.

Finally in Figure 10 we show simulated image of a solar system analog at a distance of 10pc as observed by VTPF. In contrast to OPD we now use 18 null beams distributed over a larger aperture ~ 5m. Even using conservatively a 10^{-7} null, the high spatial resolution (~ 20mas) and dynamic range (>1000) in the VTPF image allow us to detect and study Earth-size planets in the habitable zones around stars at 10pc. In the simulated image Venus, Earth, Jupiter and Saturn are clearly detected and Mars is confused by the PSFs of Earth and Venus.

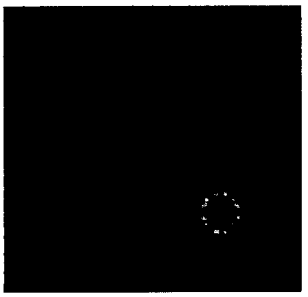

Figure 9: Simulation of a solar system analog at 10pc demonstrating VTPF imaging capability. (left) PSF for the 5m aperture synthesized by the 18 null beams. (middle) The image of the nulled star (G2V) at 10pc and solar system planets. (right) The residual image after subtracting the PSF of the nulled star. Crosses mark the planet positions. The brightest emissions are colored red.

Table 1: Required integration times with OPD for a sample of known planetary systems. *Integration times assuming Jupiter albedo and radius, except for Sun+Earth (assumes Earth albedo and radius).

Star Name	Planet mass Period (M_jup)	Semi-major Axis (AU)	Dist. (pc)	T_int (hr) (*)
Sun+Jupiter at 10 pc	1.0	5.2	10.0	26.6
Sun+Earth at 3 pc (*)	0.0031	1.0	3.0	103.4
HD160691	2.0	1.7	15.3	0.4
Ups And d	4.3	2.6	13.5	0.9
HD 10697	6.1	2.1	30.0	2.8
47 UMa c	0.8	3.7	14.1	8.5
HD 168443 c	17.0	2.9	38.5	17.0

Summary

The detection of planets outside of our solar system with a space telescope can be accomplished with modestly size apertures. Using a nulling interferometer in the pupil plane of the telescope with a coherent array of fiber optic spatial filters can achieve the diffraction control and scattering control required, and have been demonstrated in simulation experiments. The difficulty in full aperture wavefront control has been transferred to the nulling interferometer whose capabilities has been already established in previous technology demonstrations, and also eliminates extreme optical surface requirements on the primary mirror at the mid spatial frequencies. A symmetric nulling interferometer design with adjustable in spatial shear has been designed. Laboratory experiments are underway to verify this design and to verify the performance of the coherent optical fiber array.

Acknowledgement

This work was preformed at the Jet Propulsion Laboratory, California Institute of Technology, under contract to the National Aeronautics and Space Administration.

References and Bibliography

Angel, R., (1990), "Use of a 16-m Telescope to Detect Earthlike Planets," Proceedings of the Workshop on The Next Generation Space Telescope, P. Bely and C. Burrows, eds., Space Telescope Science Institute, pp. 81–94.

Angel, J.R.P, and Woolf, N.J., (1997),"An Imaging Nulling Interferometer To Study Extrasolar Planets,"Astrophysical Journal, v475, pp. 373-379.

Gaffey, M. J., J. F. Bell, and D. P. Cruikshank, (1989), Reflectance spectroscopy and asteroid surface mineralogy. In Asteroids II, Binzel et al., eds., U. Arizona Press, Tucson, pp. 128–147.

Karkoschka, E., (1994), Spectrophotometry of the Jovian planets and Titan at 300-nm to 1000-nm wavelength: The methane spectrum. Icarus, v111, 174–192.

Lee, M. & Peale S., (2001), Evolution of the GJ876 Planets into the 2:1 Orbital Resonance. BAAS, 34, 3.03

Levison, H. F., Dones, L., Canup, R., Agnor, C., and Duncan, M. J., (2001), The Role of Giant Planets in Terrestrial Planet Formation. In 32nd Annual Lunar and Planetary Science Conference, March 12–16, 2001, Houston, Texas, abstract no. 1232.

Malbet, F.,Yu, J., Shao, (1995), M., Pub Astron Soc Pacific, V107, pp. 386–398, April 1995.

Marley, and C. M. Sharp, (2000), The near-infrared and optical spectra of methane dwarfs and brown dwarfs. Astrophys. J. v531, pp. 438–446.

Meadows, V. et al., (2000), Astronomical detection of biosignatures from extrasolar planets, JPL/Caltech proposal to the NASA Astrobiology Institute CAN–00–OSS–01.

Menneson, B., and Mariotti, J.M., (1997), "Array Configurations for a Space Infrared Nulling Interferometer Dedicated to the Search for Earthlike Extrasolar Planets", Icarus, v128, pp. 202–212.

Mennesson B.,Ollivier M., and Ruilier C., (2002), "On the use of single-mode waveguides to correct the optical defects of a nulling interferometer", J. Opt. Soc. Am. A, Feb 2002.

Morgan, R., Burge, J., and Woolf, N., (2000), "Nulling Interferometric Beam Combiner Utilizing Dielectric Plates" Experimental Results in the Visible Broadband SPIE v4006.

Saumon D., Hubbard W.B., Burrows A. et al., (1996), ApJ 460, 993.

Serabyn, E., Wallace, J.K., Hardy, G.J., Schwindthin, E.G.H., and Nguyen, (1999), "Deep Nulling of Visible LASER Light", Appl. Opt., v38, p7128.

Serabyn, E. and Colavita, M.M., (2001),"Fully Symmetric Nulling Beam Combiners", Applied Optics, v40, pp. 1668–1671.

Shao, M.,(1991), "Hubble Extra Solar Planet Interferometer", SPIE v1494.

Sudarsky, D., A. Burrows, and P. Pinto. (2000), Albedo and reflection spectra of extrasolar giant planets. Astrophys. J. v538, 885--903.

Wallace, K., Hardy, G, and Serabyn, E., (2000), "Deep and stable interferometric nulling of broadband light with implications for observing planets around nearby stars", Nature, v406.

Wu, Y., and Goldreich, P., (2001), Tidal evolution of the planetary system around HD 83443. Astrophys. J. submitted

A Visible Light Terrestrial Planet Finder --Planet Detection and Spectroscopy by Nulling Interferometry with a Single Aperture Telescope

B.M. Levine, Michael Shao, C.A. Beichman, B. Mennesson, R. Morgan, G. Orton, E. Serabyn, S. Unwin, T. Velusamy,
Jet Propulsion Laboratory/California Institute of Technology
4800 Oak Grove Drive
Pasadena, CA 91109-8099
and
N. Woolf
University of Arizona, Seward Observatory, Tucson, AZ

Presented at the SPIE Interferometry in Space Conference, 26 August 2002, Waikoloa, HI

JPL
Jet Propulsion Laboratory
California Institute of Technology

Abstract

Planet detection around a bright star depends the resolution of the imaging system and the degree of light suppression of the star relative to the planet. We present a concept for a visible light Terrestrial Planet Finding (VTPF) mission. Its major feature is an imaging system for planet detection using a nulling interferometer behind a single aperture telescope. This configuration is capable of detecting earth-like planets with a 5m aperture using both imaging and spectroscopic imaging modes. We will describe the principles of the system, and show results of studies demonstrating its feasibility.

Visible Nuller Concept

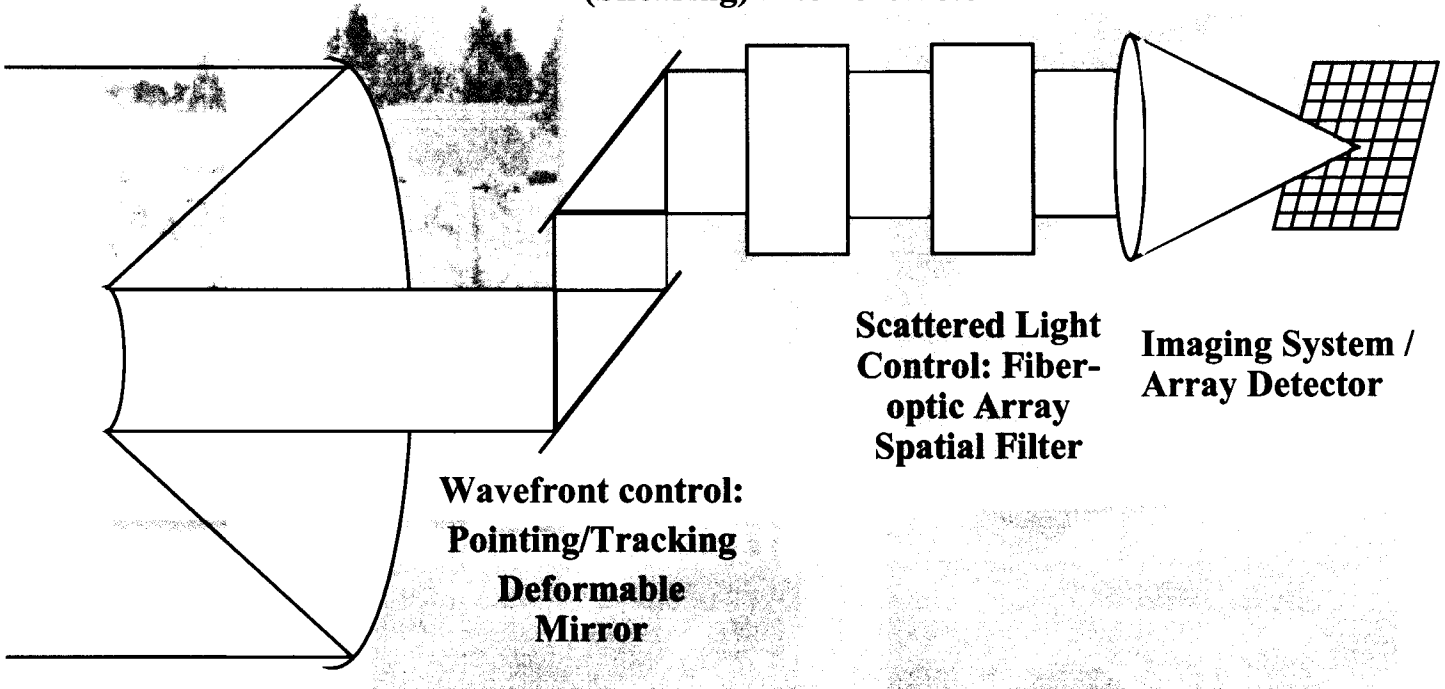

Basis for Using a Single Aperture Telescope as a Visible Nulling Interferometer

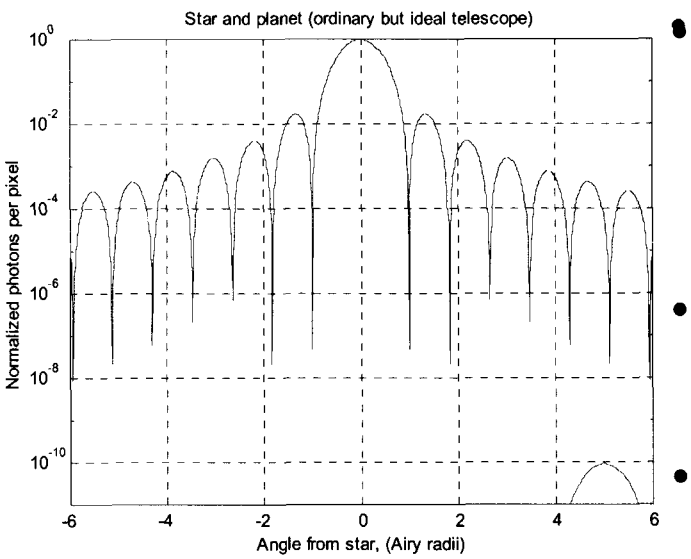

- A modest sized aperture telescope can theoretically resolve an extra-solar planet
  - Jupiters at 10 pc $b > 0.3$m (λ=0.75μm)
  - Earths at 10 pc $b > 1.5$ m
- The major issue is overcoming the contrast between star and planet (10^{-9}-10^{-10})
- Coronagraphs need to perform detection at 3rd Airy ring or greater to suppress the contrast ratio

- A nulling interferometer can perform this detection within, $\theta = \lambda/b$, $b < D$ *[(O)~1-4m]*
  - A single aperture telescope that can synthesize the minimum required baseline is capable of performing planet detection equally well if not better than a coronagraph for an equivalent diameter telescope.

JPL
Jet Propulsion Laboratory
California Institute of Technology

Critical Comparison of a Visible Nulling Nuller Interferometer to a Coronagraph

Attribute	Coronagraph	Nulling Interferometer
Telescope Design	Imaging mode	Beam Compression Cassegrain Configuration Acceptable
Telescope Primary Mirror	'Hubble' (λ/80 rms) or better minimum power in midspatial frequencies	Diffraction Limited (λ/20 rms OK)
Configuration	Unobscured Configuration Preferred	Cassegrain acceptable
Diffraction Control		
Occulter	Size, Apodization critical	na
Pupil (Lyot)	Localization (unaberrated image plane), Apodization critical	Location needed for Deformable Mirror
Nulling Interferometer	na	θ^4 null required , O(Å) Path length control for nulling and to suppress stellar leakage
Pass band	na	Dispersion correction critical for wide band nulling
Diffraction Suppression	3-4 Airy Rings (10^{-9} – 10^{-10})	λ/b (10^{-9} – 10^{-10}) adjustable
Scatterd Light Control		
Wavefront Sensor	O(Å) sensitivity (to localize pupil and to drive deformable mirror to suppress mid-spatial frequency errors)	O(20nm) sensitivity (to localize pupil and correct mirror to diffraction limit)
Pointing and Tracking	O(Å) sensitivity	O(20nm) sensitivity
Deformable Mirror	Å sensitivity over O(1000) actuators	O(20nm) sensitivity
Spatial Filter Array	na	O(100-1000) Diffraction Limited Coherent Array Required

ICE Interferometry Center of Excellence

Multi-subaperture Nuller Performance

- Leakage for a theta^4 null.
  - (left) the transmission pattern over a 1 arcsec field. (planet search mode)
  - (right) a 1 mas field, where we want to suppress the star.

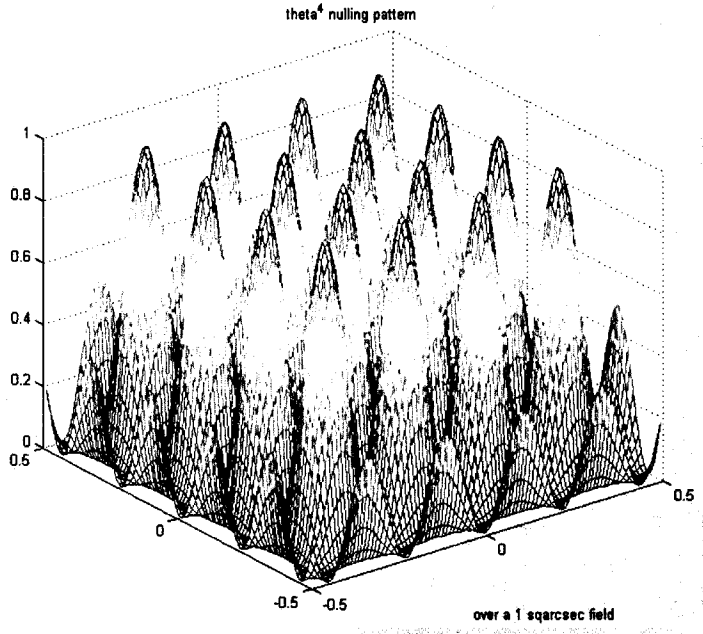

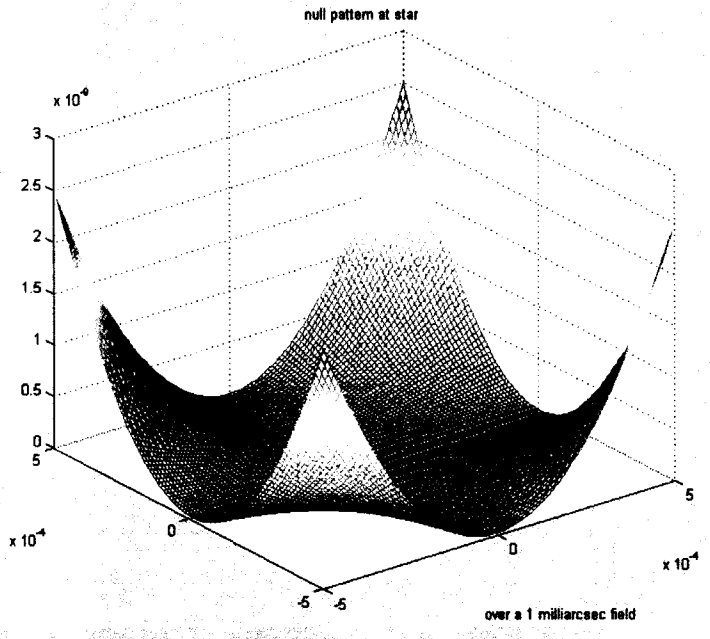

- A Sun at 10pc is 1 mas in diameter. Total leakage because of the nuller is < 1e-9 (Not yet considered for coronagraphic imaging).
- That's spread over 100 to 1000 pixels. So if we had perfect optics, the star light is suppressed to 1e-11 to 1e-12.

Symmetric Shearing Achromatic Nulling Interferometer (Shao and Serabyn)

- **Preserves pupil orientation and polarization**
- **Broadband null--Calculation for nulling depth for common optical glasses, BK7 and Fused Silica.**

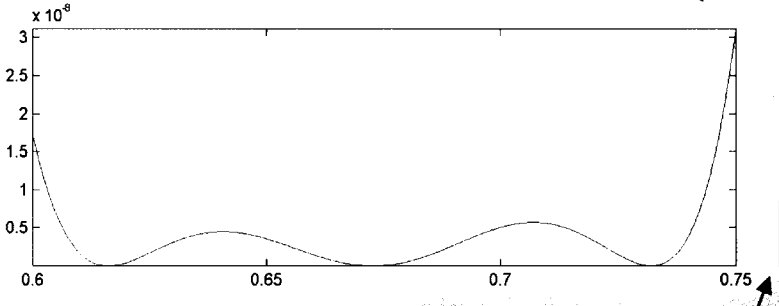

- Δt,BK7 = 391.687 +/- 0.052 um
- Δt, F.S. = 479.189 +/- 0.057 um
- Delay = 104.921 um

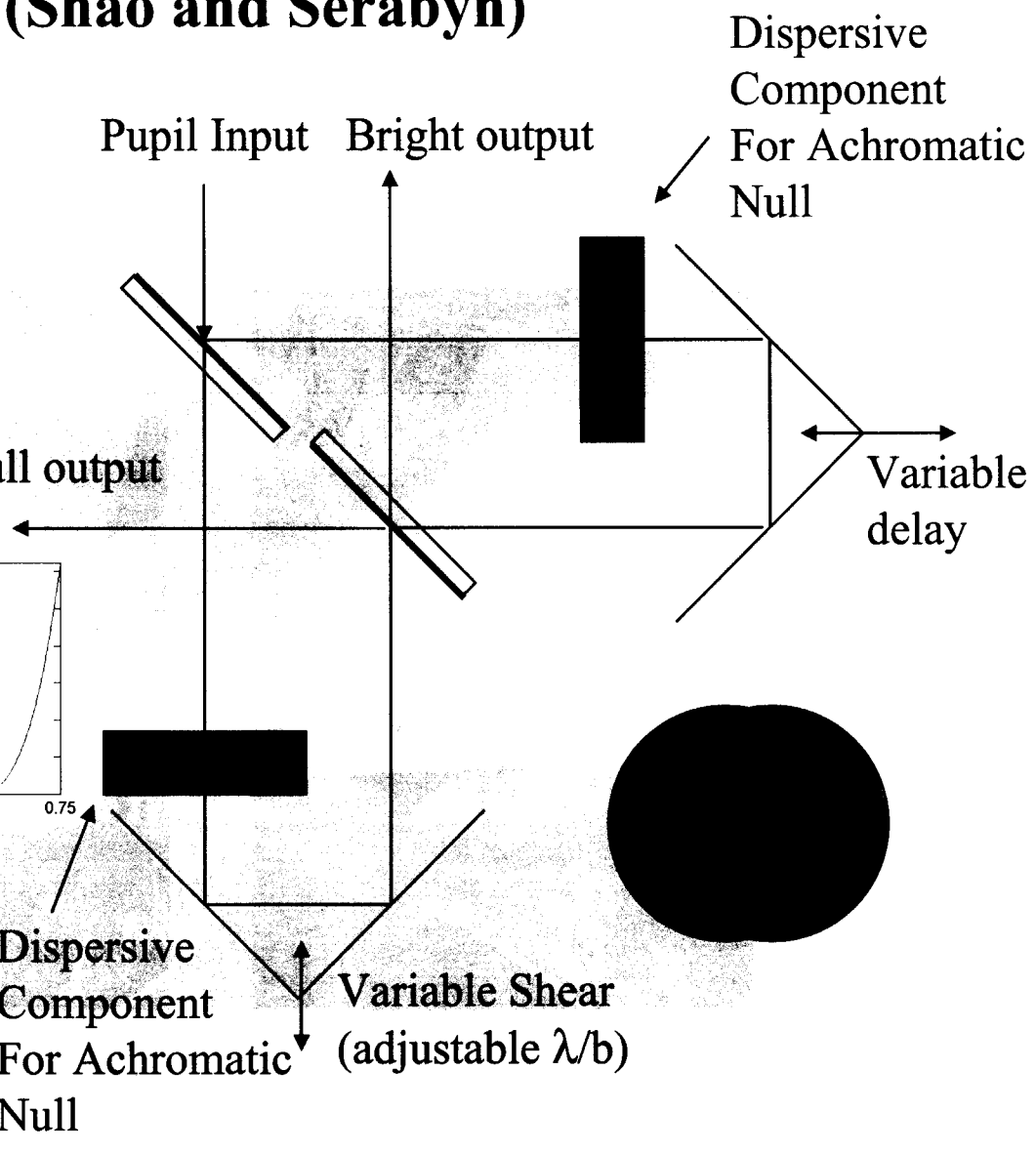

Visible Nulling System Concept

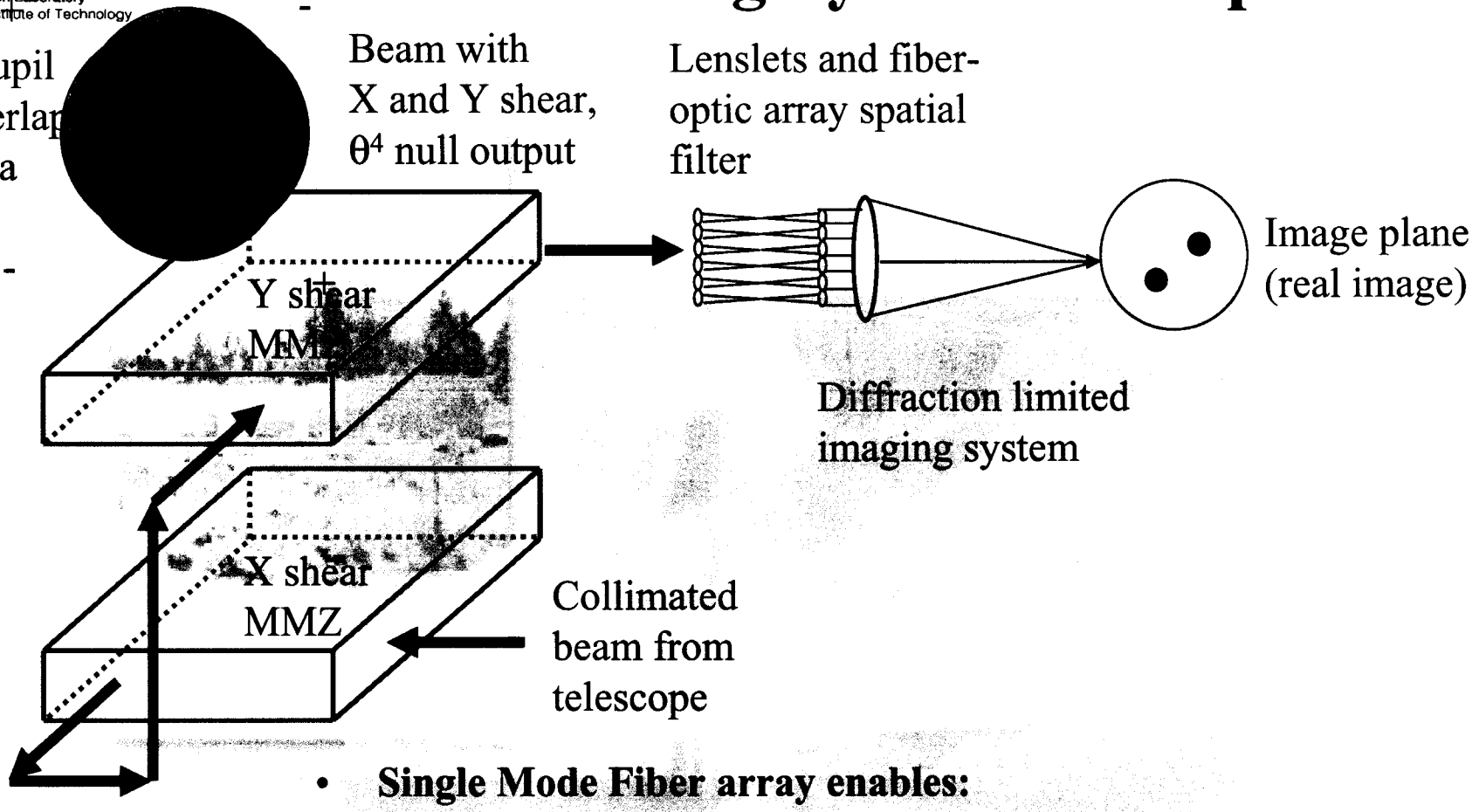

- **Single Mode Fiber array enables:**
  - **10^-9 suppression achieved with 10^-7 nuller and 100 lenslets**
  - **Multiple sub-apertures make the detection less susceptible to Exo-Zodiacal Dust**
    - **Residual background is incoherent with planet image**
    - **Preserves field of view**

Jet Propulsion Laboratory
California Institute of Technology

Integration Time Calculations

- **Integration times for SNR=5**
  - **For a Jupiter sized planet the integration time goes as:**

$$T_{int} = 14.3\ hr\ .\left(\frac{SNR}{5}\right)^2.\left(\frac{1.5}{D}\right)^2.\left(\frac{0.05}{eff}\right).\left(\frac{sl}{10^{-8}}\right).\left(\frac{Dist_{in\,pc}}{10}\right)^2.\left(\frac{Reso}{1.4}\right).\left(\frac{Sep}{5.2}\right)^4.\left(\frac{F_{sun}}{F^*}\right)$$

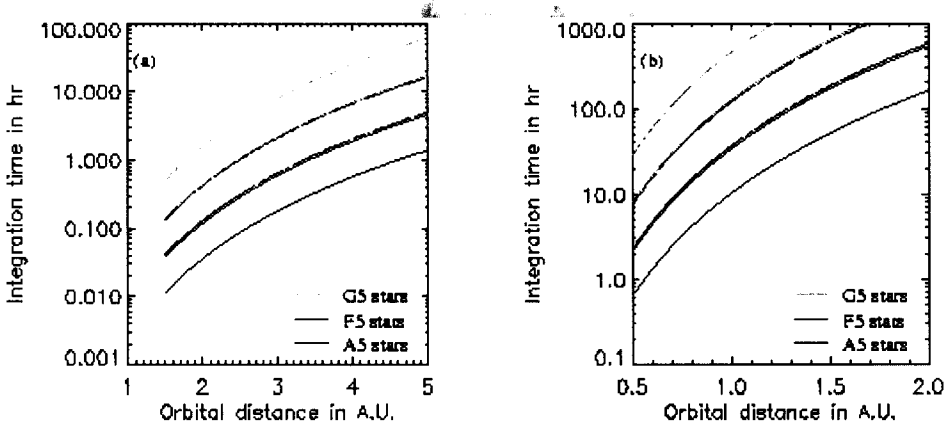

(a): Integration times for 5σ detection of Jupiter analogs around main sequence stars of various spectral types located 10pc away. Plain curve: broad band (500-1000 nm) detection. Dotted curves: narrow band ($R \sim 20$) detection. Reso=, the spectral resolution. Telescope diameter, *D*, is 1.5m, *eff*, the overall optical efficiency (including primary area filling factor, optics transmission and detector quantum efficiency) is 5%, interferometric off-axis point-source transmission is 25%. The fraction of stellar leakage, *sl*, at planetary location: 10-8. *Dist* is the stellar distance in pc, *Sep*, is the star-planet separation in AU, and *F* denotes the appropriate stellar flux. (b): Similar plot for Earth-like planets using a 4m telescope. Solid lines denote imaging. The broken lines denote spectroscopic observations.

Required integration times with OPD for a sample of known planetary systems. *Integration times assuming Jupiter albedo and radius, except for Sun+Earth (assumes Earth albedo and radius).

Star Name	Planet mass Period (M_jup)	Semi-major Axis (AU)	Dist. (pc)	T_int (hr) (*)
Sun+Jupiter at 10 pc	1.0	5.2	10.0	26.6
Sun+Earth at 3 pc (*)	0.0031	1.0	3.0	103.4
HD160691	2.0	1.7	15.3	0.4
Ups And d	4.3	2.6	13.5	0.9
HD 10697	6.1	2.1	30.0	2.8
47 UMa c	0.8	3.7	14.1	8.5
HD 168443 c	17.0	2.9	38.5	17.0

Imaging Simulations

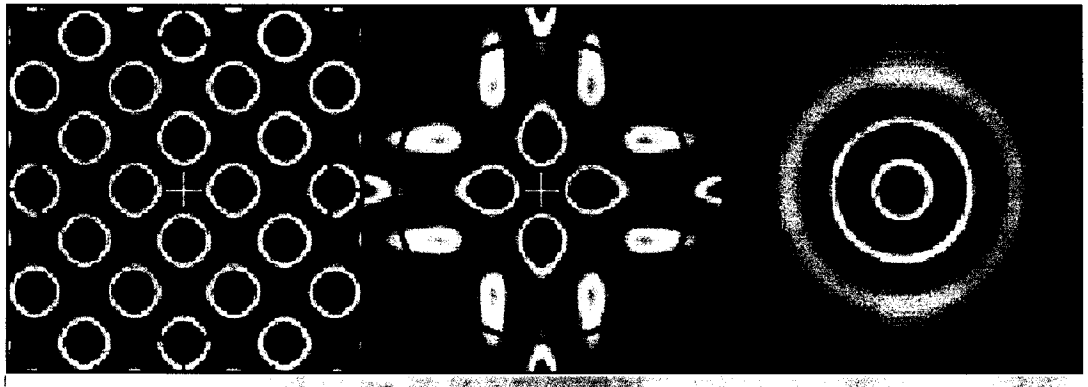

The null response pattern of a 1.5m precursor . (left) at wavelength 650nm and at one orientation. (middle) Using wavelengths 500-1000nm and at one orientation.(right) Using wavelengths 500-1000nm and combining all orientations 0-360deg orientations 0-360deg. The circle represents 5AU radius at 10pc distance. Response maxima are shown in red.

Simulations of observed planet fluxes compared to the PSF of the stellar leak as a function of the planet distance. The planet flux densities are assumed to be that for Jupiter size and given in units of stellar flux Null depth of 10-7 was assumed, and the planet fluxes are averaged over all orientations of the null pattern.

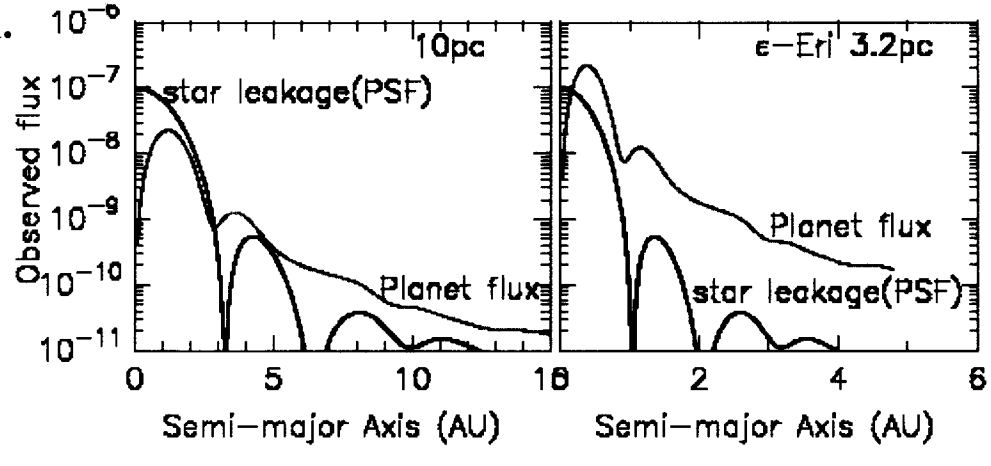

Ultimate VTPF Imaging Capability

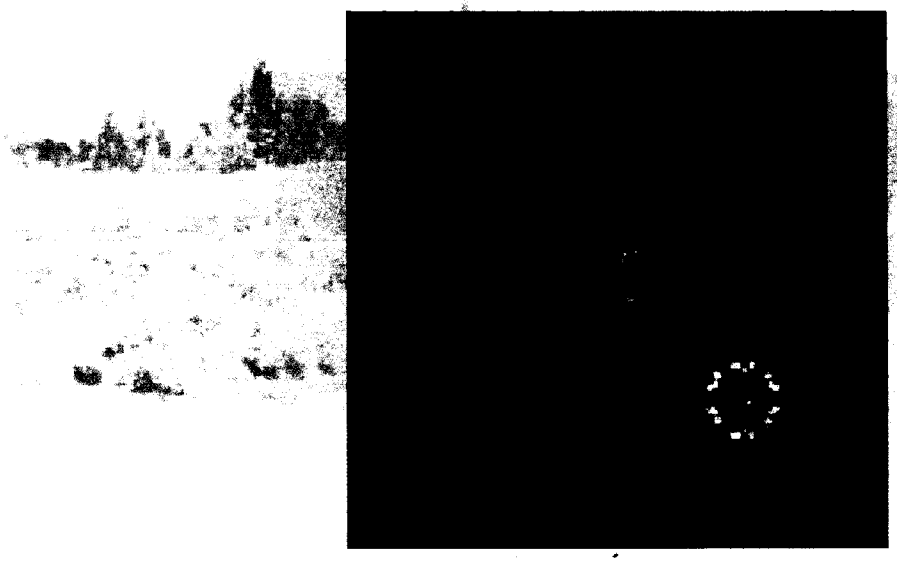

(for the 4m aperture synthesized by the 18 null beams. The image of the nulled star (G2V) at 10pc and solar system planets. The brightest emissions are red.

Planetary Spectroscopy with Visible Nuller

- **The spectrum of Earth shows evidence of atmospheric scattering in the rise of the spectrum going from 600 down to 500nm. This spectrum shows critical signatures in NASA's search for evidence of life:**

(i) water vapor absorption bands at 920nm (with fainter ones at 720 and 820m),

(ii) a narrow band of O2 near 760nm that could be resolved,

(iii) a spectral "vegetation edge" rising from 600 to 700nm which is due to absorption by green foliage.

- **(Low resolution) Spectroscopy is capable of discriminating these features**

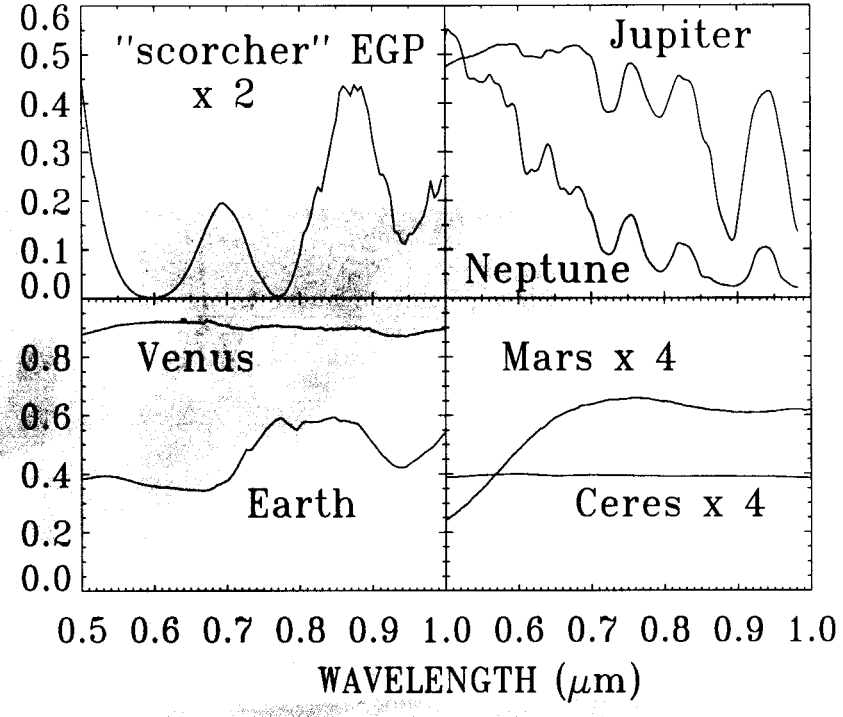

With a precursor of 1.5m diameter and then a full scale TPF at 4m diameter, one could easily envision re-visiting a planet showing water, oxygen and hints of vegetation for extra signal, leading to confirmation of these features.

JPL
Jet Propulsion Laboratory
California Institute of Technology

Excellence

Summary

- **Planet detection concept using visible light with**
  - **Modest sized single aperture telescope**
  - **Nulling interferometer/Coherent fiber optic array**
- **Concept is scalable to perform the TPF mission using current technology**
  - **Capable of imaging and spectroscopy of Jupiter-like planets and Earth-like planets**
- **Status**
  - **Nulling fiber array imager to be demonstrated in the laboratory**